

## Stabilization of Barstar by Chemical Modification of the Buried Cysteines

S. Ramachandran and Jayant B. Udgaonkar\*

National Centre for Biological Sciences, TIFR Centre, P.O. Box 1234, Indian Institute of Science Campus, Bangalore 560012, India

Received January 11, 1996; Revised Manuscript Received April 23, 1996<sup>⊗</sup>

**ABSTRACT:** The internal packing of residues in the small monomeric protein barstar was severely perturbed by chemical modification of the two buried cysteine residues with the thiol reagent 5,5'-dithiobis(2-nitrobenzoic acid) (DTNB) after prior unfolding of the protein using guanidine hydrochloride (GdnHCl). The modification produces mixed disulfides between 5-thio(2-nitrobenzoic acid) and the two Cys residues. To understand the effects of the modification of the individual cysteine residues, Cys40 and Cys82, the modification was also carried out on the two single Cys→Ala mutant forms of barstar, C40A and C82A, whose structures, activities, and stabilities were first shown to be similar to those of *wt* barstar. Equilibrium GdnHCl-induced denaturation studies on *wt* barstar show that the modification causes the midpoint of the denaturation curve to increase by 0.6 M and the stability to increase by 1.3 kcal mol<sup>-1</sup>. Both C40A and C82A also denature at higher concentrations of GdnHCl after modification. Modification of Cys40 has approximately the same stabilizing contribution as does modification of Cys82. The structures of the modified and unmodified proteins have been compared using circular dichroism (CD) spectroscopy, UV difference absorption spectroscopy, and fluorescence spectroscopy. It is shown that the 5-thio(2-nitrobenzoic acid) groups introduced by reaction with DTNB are buried in hydrophobic environments in the modified C40A and C82A mutant proteins, as well as in modified *wt* barstar. The far-UV CD spectra of the modified and unmodified proteins are similar, but the mean residue ellipticity at 220 nm of *wt* barstar is reduced by 30% upon modification. Such a decrease is not seen for either C40A or C82A. The barnase-inhibiting activities of the three modified proteins are shown to be similar to those of the corresponding unmodified proteins. Thus, the severe perturbations of the internal packing, which result in a significant increase in stability, do not appear to affect the overall fold of barstar.

Only a few rational methods exist for increasing protein stability. A recent strategy is based on the recognition that tight packing of buried residues in a protein is an important determinant of protein stability (Baldwin & Matthews, 1994; Hubbard & Argos, 1995; Richards & Lim, 1993). Thus, an important structural feature distinguishing proteins from thermophilic organisms from their homologous counterparts in mesophilic organisms appears to be even more compactness and efficient packing of hydrophobic residues (Russell & Taylor, 1995). Engineering an increase in packing density through mutagenesis has been reported to lead to greater stability in the case of ribonuclease H1 (Ishikawa *et al.*, 1993), T4 lysozyme (Anderson *et al.*, 1993), and  $\lambda$  repressor (Lim *et al.*, 1992, 1994). The general applicability of such a strategy to increase protein stability rests on the ability to correctly predict possible adjustments of both the side chain and the main chain (Baldwin & Matthews, 1994; Richards & Lim, 1994), and the difficulty lies in improving upon the already very high packing densities found in the interiors of most proteins (Richards, 1977).

The value of the small monomeric protein barstar as a model protein for protein folding studies is well established. Barstar is produced naturally in the bacterium *Bacillus amyloliquefaciens*, where it functions as the intracellular

inhibitor of the ribonuclease, barnase (Hartley, 1988). The 89 amino acid residue polypeptide chain of barstar folds into a structure comprising four  $\alpha$ -helices and a three-stranded parallel  $\beta$ -sheet (Guillet *et al.*, 1993; Lubienski *et al.*, 1994). Kinetic studies have shown that *wt* barstar<sup>1</sup> folds via three folding pathways defined by multiple folding intermediates (Shastry *et al.*, 1994; Shastry & Udgaonkar, 1995), and that an initial nonspecific hydrophobic collapse facilitates subsequent formation of secondary and tertiary structure (Agashe *et al.*, 1995). Barstar adopts a molten globule-like conformation at low pH (Khurana & Udgaonkar, 1994; Swaminathan *et al.*, 1994) which forms a large soluble oligomer (Khurana *et al.*, 1995).

Several lines of study have suggested that the interior of barstar is more loosely packed than the interiors of other proteins. Extensive thermodynamic studies (Agashe & Udgaonkar, 1995; Khurana *et al.*, 1995) have shown that the denaturation of barstar is characterized by an extremely low enthalpy change and a relatively high heat capacity change (Agashe & Udgaonkar, 1995), which have been correlated with a relatively poorly packed hydrophobic interior (Wintrode *et al.*, 1995). Aromatic ring flipping of Phe74 in the hydrophobic core has been observed in NMR

<sup>†</sup> This work was funded by the Tata Institute of Fundamental Research and by the Department of Biotechnology, Government of India.

\* Corresponding author. FAX: 91-80-3343851. E-mail: jayant@ncbs.tifrbng.res.in.

<sup>⊗</sup> Abstract published in *Advance ACS Abstracts*, June 1, 1996.

<sup>1</sup> Abbreviations: C40A, the Cys40→Ala40 mutant form of barstar; C82A, the Cys82→Ala82 mutant form of barstar; C40AC82A, the Cys40Cys82→Ala40Ala82 double mutant form of barstar; *wt* barstar, wild-type barstar; GdnHCl, guanidine hydrochloride; DTNB, 5,5'-dithiobis(2-nitrobenzoic acid); TNB, 5-thio(2-nitrobenzoic acid); 4-PDS, 4,4'-dithiopyridine; DTT, dithiothreitol; BME,  $\beta$ -mercaptoethanol; CD, circular dichroism.

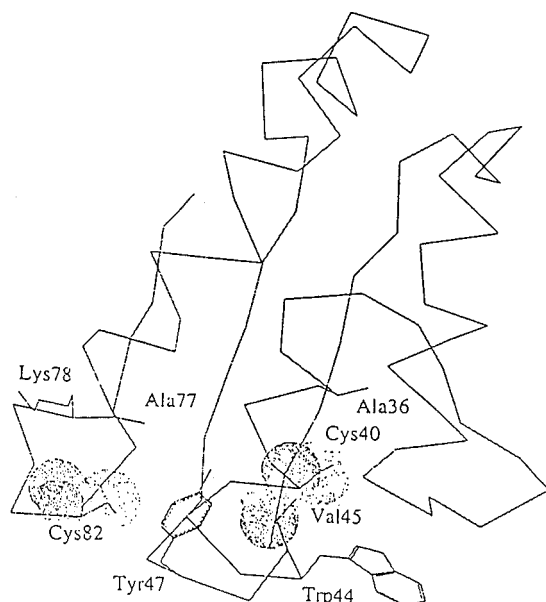


FIGURE 1: Structural environments of Cys40 and Cys82 in barstar. The figure was made using the program Insight II and the coordinates (pdb1bta.ent) of the solution structure of barstar (Lubienski *et al.*, 1994).

studies (Lubienski *et al.*, 1994). Hydrogen exchange experiments (A. Bhuyan, unpublished observations) also indicate that the structure of barstar is unusually flexible. Barstar is therefore a suitable protein to study how structural rearrangements of side chains as well as the main chain occur in a protein, when protein engineering is used to increase stability by increasing packing density. Moreover, the evolution of barstar appears to have optimized its function and not its stability (Schreiber *et al.*, 1994), suggesting that it should be possible to engineer significant increases in stability.

Cysteine residues are usually buried in proteins (Rose *et al.*, 1985). The thiol groups of buried cysteine residues can be easily and specifically modified by a large number of thiol reagents (Brocklehurst, 1979; Wynn & Richards, 1993) after prior unfolding of the protein. Thus, chemical modification of buried cysteines is a convenient method of perturbing the packing of buried residues in a protein. Moreover, the introduction of unnatural amino acids into the hydrophobic core may make it easier to improve the high packing densities that have evolved in the structures of proteins (Mendel *et al.*, 1992). The methodology is suitable for application to barstar, which has two buried cysteine residues (Guillet *et al.*, 1993; Lubienski *et al.*, 1994). Cys40, which is 95% buried, is located in helix 2, which along with the loop connecting helices 1 and 2 forms the region of barstar that binds to barnase (Buckle *et al.*, 1994). Cys82, which is 75% buried, is located in the loop between helix 4 and the last strand of the three-stranded  $\beta$ -sheet. The thiol group of Cys40 appears to interact weakly with Trp44 and Val45 (Figure 1) and may be forming a hydrogen bond with the main chain carbonyl of Ala36. Cys82 appears to interact with Lys78, Tyr47, and Ala77 (Figure 1).

Here we first demonstrate that the cysteine sulfhydryl groups are indeed buried in the protein in solution and do not form a Cys40–Cys82 disulfide bond. We show that earlier uncertainty (Hartley, 1989; Schreiber & Fersht, 1993) about the presence or absence of a disulfide bond arose because of the formation of mixed disulfides during the

purification of the protein. Next, we show that the structures, activities and stabilities of the cysteine mutant proteins C40A (in which Cys40 is mutated to Ala) and C82A (in which Cys82 is mutated to Ala) are similar to those of *wt* barstar. Finally, we use the common thiol reagent DTNB to chemically modify the two cysteines together in *wt* barstar and individually in the mutant proteins, C40A and C82A. The structural and energetic consequences of such chemical modification, which attaches the bulky, charged aromatic group TNB to either or both cysteines, have been studied. We have chosen to chemically label the cysteines with TNB rather than mutate them to aromatic residues, because the TNB labels on the proteins can be spectroscopically distinguished from the aromatic residues of the protein. Spectroscopic measurements indicate that the TNB labels are buried within hydrophobic environments in the proteins. It is demonstrated that barstar is significantly stabilized by DTNB modification of either cysteine thiol, even though its structure and activity appear not to be significantly altered.

## MATERIALS AND METHODS

**Chemicals.** GpG, *Torula* RNA, chromatographic resins, DTNB, 4-PDS, BME, and GdnHCl were obtained from Sigma.

**Bacterial Strains and Plasmids.** The *Escherichia coli* strain used for protein expression was MM294 (*supE44 hsdR endA1 pro thi*). The barnase expression plasmid, pMT416, and the barstar expression plasmids, pMT316 for *wt* barstar, pMT641 for C40A, and pMT642 for C82A, were kindly provided by R. W. Hartley (1988). All mutations were confirmed by dideoxy sequencing of the entire mutant barstar genes (Sanger *et al.*, 1977).

**Purification of Barstar.** The procedure for purification of barstar was as reported previously by Khurana and Udgaonkar (1994). Unless otherwise stated, BME was omitted from all buffers during purification.

**Purification of Barnase.** A 100-mL overnight culture of pMT416/MM294 was used to inoculate 1 L of rich buffered medium (containing 12 g of bactotryptone, 24 g of yeast extract, 5 mL of glycerol, 12.2 g of potassium monohydrogen phosphate, and 2.4 g of potassium dihydrogen phosphate). Barnase production was induced 18 h after inoculation by the addition of 10 mg of IPTG. Barnase was extracted by adding acetic acid to a final concentration of 5%. The cells were removed by centrifugation. The supernatant was diluted 3-fold in double-distilled water, after which SP Trisacryl was added to it. The suspension was stirred until all of the barnase was bound to it. The resin was then packed into a column, and the barnase was eluted using 2 M ammonium acetate buffer at pH 5.0. After a 10-fold dilution, the pool was loaded on a cyanogen bromide-activated Sepharose 4B column that had barstar covalently bound to it. The column was then washed with buffers in the following order: 0.1 M ammonium acetate, 1 mM EDTA, pH 8.0; 1 M ammonium acetate, 1 mM EDTA, pH 8.0; 1 mM EDTA, pH 8.0, and again with 0.1 M ammonium acetate, 1 mM EDTA, pH 8.0. The barnase was eluted with 6 M GdnHCl, 0.1 M ammonium acetate, 1 mM EDTA, pH 8.0. GdnHCl was removed on a Pharmacia fast desalting column (HR 10/10).

The purity of each protein preparation was checked by SDS–PAGE (Schagger & von Jagow, 1987). The *wt* barstar,

its mutant forms, and barnase were found to be >98% pure. Protein concentrations were determined using the Bradford assay (Bradford, 1976). The extinction coefficients of *C40A* and *C82A* in both modified and unmodified forms were found to be the same as that of *wt* barstar, namely, 23 000 M<sup>-1</sup> cm<sup>-1</sup> (Khurana & Udgaonkar, 1994).

**Inhibition Assay for Barstar.** Barstar was assayed by measuring its inhibition of barnase hydrolysis of GpG (Nath & Udgaonkar, 1995). The concentration of GpG used in the assays was 100 μM and was estimated from the change in extinction coefficient at 280 nm ( $\Delta\epsilon_{280} = 1500 \text{ M}^{-1} \text{ cm}^{-1}$ ) on degradation by barnase. The substrate dissolved in buffer (50 mM MOPS, 1 mM EDTA, pH 7.0) was equilibrated at 25 °C for 2 min in a cuvette. Appropriately diluted barnase and barstar were mixed outside, incubated at 25 °C for 2 min, and added to the cuvette. The hydrolysis of GpG was monitored at 280 nm in a Cary 1 spectrophotometer. The concentration of barnase was 1 μM for all assays, and that for *wt* barstar and the mutant proteins was 0.5 μM.

**Thiol Assays.** Thiol assays were performed both on fully folded protein in 100 mM sodium phosphate buffer at pH 7.3 containing 1 mM EDTA and on unfolded protein in the same buffer containing 6 M GdnHCl. For some assays, the protein was reduced prior to assay by incubation in the presence of 5 mM DTT for 1 h after which the DTT was removed on a G-25 gel filtration column. The thiol reagent (DTNB or 4-PDS) was added to a final concentration of 300 μM. The protein concentration was 3 μM for all assays. In the DTNB assays, the number of free thiols per barstar molecule was determined by determining the number of TNB anions released by measurement of the absorbance at 412 nm. A value of 14 150 M<sup>-1</sup> cm<sup>-1</sup> was used for the extinction coefficient of the TNB anion in the absence of GdnHCl, and a value of 13 700 M<sup>-1</sup> cm<sup>-1</sup> was used for the extinction coefficient in 6 M GdnHCl (Ellman, 1959; Riddles *et al.*, 1983). In the PDS assays, the number of free thiols was determined by determining the amount of product, 4-thiopyridone (4-TP) formed by measurement of the absorbance at 324 nm. A value of 19 600 M<sup>-1</sup> cm<sup>-1</sup> was used for the extinction coefficient of 4-TP (Grasseti & Murray, 1967; Liang & Terwilliger, 1991).

**Preparation of DTNB-Modified Barstar.** 2.5 mL of 6 mM DTNB in 6 M GdnHCl, 100 mM phosphate buffer at pH 8.0 was added to 6 mg of barstar (*wt* or mutant protein). The reaction of DTNB with the cysteine(s) proceeded for 2 min. The reaction mixture was then passed through a PD10 column that had been equilibrated with 20 mM phosphate buffer, 0.25 mM EDTA at pH 7.0, to remove out the GdnHCl, excess DTNB and the TNB<sup>-1</sup> anion released in the reaction of the cysteines with DTNB. The completion of the reaction was checked by adding DTT to the labeled protein after unfolding it in 6 M GdnHCl, and measuring the absorbance at 412 nm. The *wt* barstar was labeled to the extent of 2 TNB labels/protein molecule, and the *C40A* and *C82A* mutant proteins were each labeled to the extent of 1 TNB label/protein molecule.

**Spectroscopic Characterization.** CD spectra were collected on a Jasco J720 spectropolarimeter. Spectra were collected with a bandwidth of 1 nm, response time of 1 s, and a scan speed of 20 nm/min. Each spectrum was an average of at least 5 scans. The protein concentrations used were 2 and 20 μM for far- and near-UV CD spectra, respectively. The cuvette path length was 1 cm in both cases.

Fluorescence spectra were collected on a Spex spectrofluorimeter. The protein was excited at 287 nm, and emission was monitored from 300 to 400 nm, with a bandwidth of 1 nm for excitation and 2 nm for emission. The protein concentration was typically 2 μM, and the pathlength of the cuvette was 1 cm.

**GdnHCl-Induced Equilibrium Denaturation Studies.** Far-UV CD was used to monitor equilibrium unfolding. Varying concentrations of GdnHCl were added in isothermal GdnHCl-induced denaturation studies. The protein was equilibrated for at least 15 h before measurement. 1 mM DTT was added in studies carried out in reducing conditions. All buffers were passed through 0.22 μm filters and degassed before use. The concentration of the GdnHCl stock solution was checked by measurement of the refractive index (Pace *et al.*, 1989). CD data were collected on a Jasco J720 spectropolarimeter using a cuvette of 0.2 cm path length. Spectra were collected using a bandwidth of 1 nm, a response time of 1 s, and a scan speed of 20 nm/min. Each spectrum was the average of 10 scans. The protein concentration used was typically 10 μM.

**Thermally-Induced Denaturation Studies.** Thermally-induced denaturation studies were carried out in 20 mM sodium phosphate, 1 mM EDTA buffer at pH 7. Temperature melts were carried out using far-UV CD at 220 nm as a probe for folding. The protein was equilibrated at each temperature for 6 min. Spectra were collected using a bandwidth of 1 nm, a response time of 1 s, and a scan speed of 20 nm/min. Each spectrum was an average of 15 scans.

**Gel Filtration Experiments.** Size exclusion chromatography was done on barstar in the native and unfolded forms, in the presence of GdnHCl, under reducing and non-reducing conditions. A Superdex 75 HR10/30 column was used with a Pharmacia FPLC system. The column was equilibrated with the buffer by passing four column volumes of the appropriate buffer through it prior to injecting 50 μL of a 20 μM protein solution. A flow rate of 0.7 mL/min was used.

**Data Analysis.** Raw GdnHCl-induced equilibrium denaturation data were first converted to plots of  $f_U$ , the fraction of protein in the unfolded state, versus [D] using eq 1

$$f_U = \frac{Y_O - (Y_F + m_F[D])}{(Y_U + m_U[D]) - (Y_F + m_F[D])} \quad (1)$$

where  $Y_O$  is the value of the spectroscopic property being measured at a denaturant concentration [D].  $Y_F$  and  $Y_U$  represent the intercepts, and  $m_F$  and  $m_U$  represent the slopes of the native and the unfolded base lines, respectively.

$f_U$  is related to the free energy of unfolding,  $\Delta G_U(D)$ , by a transformation of the Gibbs–Helmholtz equation in which the equilibrium constant for unfolding in the folding transition zone,  $K_{app}$ , is given by  $K_{app} = f_U/(1 - f_U)$ .

$$f_U = \frac{e^{-(\Delta G_U + m_G[D])/RT}}{1 + e^{-(\Delta G_U + m_G[D])/RT}} \quad (2)$$

The linear dependence of  $\Delta G_U(D)$  on denaturant concentration has been previously demonstrated (Agashe & Udgaonkar, 1995):

$$\Delta G_U(D) = \Delta G_U + m_G[D] \quad (3)$$

$\Delta G_U$  and  $m_G$  are therefore the intercept and the slope, respectively, of the plot of  $\Delta G_U(D)$  versus denaturant concentration.  $\Delta G_U$  corresponds to the free energy difference between the folded and unfolded states in the absence of any denaturant, and  $m_G$  is a measure of the cooperativity of the unfolding reaction. The concentration of denaturant at which the protein is half unfolded [when  $\Delta G_U(D) = 0$ ] is given by  $C_m$ , and from eq 3,  $\Delta G_U = -C_m m_G$ .

## RESULTS

*wt Barstar Has No Disulfide Bond.* The *wt* barstar that had been purified using buffers that did not contain BME was unfolded in 6 M GdnHCl, and the unfolded protein was assayed for the presence of thiol groups (see Methods). Two thiol groups were determined to be present per barstar molecule (data not shown). Thus, the two cysteine residues of barstar (Hartley, 1988) do not form a disulfide bond.

When a similar assay on unfolded barstar was, however, performed on preparations of the protein that had been purified using buffers that contained 5 mM BME, the number of thiol groups per barstar molecule was found to vary between 1.2 and 1.6. If such protein samples were, however, first reduced by 1 mM DTT in the presence of 6 M GdnHCl, and the DTT completely removed by gel filtration, the thiol assay detected two cysteine thiol groups per molecule of barstar.

*The Two Thiol Groups Have Low Water Accessibility in the Folded Protein.* Figure 2A shows the time course of reaction of the thiol reagent, 4-PDS with the thiol groups in fully folded *wt* barstar, which had been purified using buffers that did not contain BME. The assay shows that there are two free cysteine thiol groups per molecule of barstar. The reaction of 4-PDS with these thiol groups is slow and takes approximately 30 min to reach completion. Figure 2A also shows that the kinetics of the reactions with *C40A* and *C82A* are similar to those with *wt* barstar, and in each case one free cysteine thiol group per protein molecule is detected. Figure 2B shows the kinetics of the reactions of DTNB with fully folded *wt* barstar, *C40A*, and *C82A*. In all cases, the DTNB reaction is even slower than the 4-PDS reaction, and after 10 h only 1.5 thiol groups in *wt* barstar and 0.7 thiol groups in either *C40A* or *C82A* have reacted with DTNB. In contrast, when *wt* barstar (3  $\mu$ M) is completely unfolded in 6 M GdnHCl, the thiol groups react completely with 300  $\mu$ M DTNB with an apparent time constant of 1 s (data not shown).

*Stability of wt Barstar Is the Same in Reducing and Non-Reducing Conditions.* Figure 3A shows thermal denaturation curves of barstar obtained under both reducing and non-reducing conditions. Both curves are coincident, suggesting that there is no difference in the stability of *wt* barstar under reducing or non-reducing conditions.

Figure 3B shows GdnHCl-induced denaturation curves of barstar obtained under both reducing and non-reducing conditions. Also shown in Figure 3B, are the GdnHCl-induced denaturation curves obtained, under both reducing and non-reducing conditions, for *wt* barstar that had been purified using buffers containing BME and for which the number of free thiol groups per barstar molecule had been determined to be 1.5. All four denaturation curves are coincident. Thus, the stability of *wt* barstar is the same in both reducing and non-reducing conditions. Moreover, the

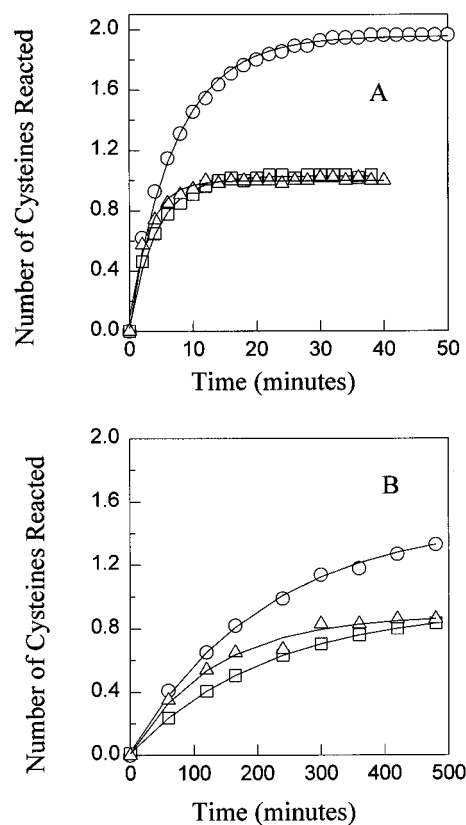


FIGURE 2: 4-PDS and DTNB assays of the thiols in fully-folded *wt* barstar (○), *C40A* (□) and *C82A* (△). The DTNB assay was done at pH 7.3, and the 4-PDS assay was done at pH 7.0. The number of thiol groups detected is plotted against time of reaction. (A) 4-PDS assay. The 4-PDS assay shows that there are two thiols per *wt* barstar molecule and one each in each *C40A* and *C82A* molecule, which take 30 min to react completely. (B) DTNB assay. Only 1.5 thiols per *wt* barstar molecule react in 10 h, and 0.8 thiols per *C40A* or *C82A* molecule.

presence of mixed disulfides at one in four thiol groups does not appear to affect stability.

*Spectroscopic Characterization, Activities, and Stabilities of the Cys→Ala Mutants of Barstar.* Table 1 shows that the activities and mean residue ellipticities at 220 and 275 nm of the two single *Cys→Ala* mutant proteins are similar to those of *wt* barstar. For both mutant proteins, the wavelength of maximum fluorescence emission of the fully folded state increases to 337 nm compared to the value of 334 nm for *wt* barstar (Table 1) but remains at 356 nm for the fully unfolded state in 6 M GdnHCl. The fluorescence intensities are higher for the mutant proteins in both the folded and unfolded states. The difference UV absorbance spectra (Figure 6) of the mutant proteins are similar to those of *wt* barstar. The unfolding reactions of *C40A*, *C82A*, and *wt* barstar are accompanied by changes in  $\epsilon_{287}$  of 1300, 1800, and 1400  $M^{-1} cm^{-1}$ , respectively. The spectroscopic properties of the single *Cys→Ala* mutant proteins are similar to those of *C40A**C82A*, the double cysteine mutant protein, which have been reported earlier (Khurana *et al.*, 1995).

The stabilities of *wt* barstar and its two single *Cys→Ala* mutants were determined from GdnHCl-induced denaturation curves obtained using mean residue ellipticity (a probe for secondary structure) and intrinsic *trp* fluorescence at 322 nm (a probe for tertiary structure) to follow the unfolding reaction. For each protein, both probes gave identical values for the midpoint ( $C_m$ ) of the denaturation curve (Table 2).

Table 1: Effect of DTNB Modification on the Structures and Activities of *wt* Barstar and the Cys→Ala Mutant Proteins at pH 7, 25 °C

protein	relative activity <sup>a</sup>	mean residue ellipticity <sup>b</sup>		UV absorbance, <sup>c</sup> $\Delta\epsilon_{287}$	fluorescence <sup>d</sup>	
		$\Theta_{220}$	$\Theta_{275}$		$F_{\max}$ (- GdnHCl)	$F_{355}$ (+ 6 M GdnHCl)
<i>wt</i> barstar	1.0	-14 800 ± 500	-230 ± 20	1400 ± 150	1.0	0.81
<i>C40A</i>	1.0	-13 800 ± 150	-195 ± 30	1300 ± 150	1.14	0.86
<i>C82A</i>	1.1	-13 100 ± 400	-190 ± 20	1800 ± 150	1.04	0.85
2NTB- <i>wt</i> barstar	0.8	-10 300 ± 300	-23 ± 6	3600 ± 150	0.07	0.24
1NTB- <i>C40A</i>	1.1	-13 400 ± 400	-135 ± 20	2000 ± 150	0.18	0.67
1NTB- <i>C82A</i>	1.0	-12 300 ± 200	18 ± 10	3100 ± 150	0.15	0.23

<sup>a</sup> All activities are relative to a value of 1.0 for *wt* barstar. <sup>b</sup> In deg cm<sup>2</sup> dmol<sup>-1</sup>. <sup>c</sup> In M<sup>-1</sup> cm<sup>-1</sup>. <sup>d</sup> All fluorescence intensities are relative to a value of 1.0 for the fluorescence of *wt* barstar in the absence of GdnHCl.

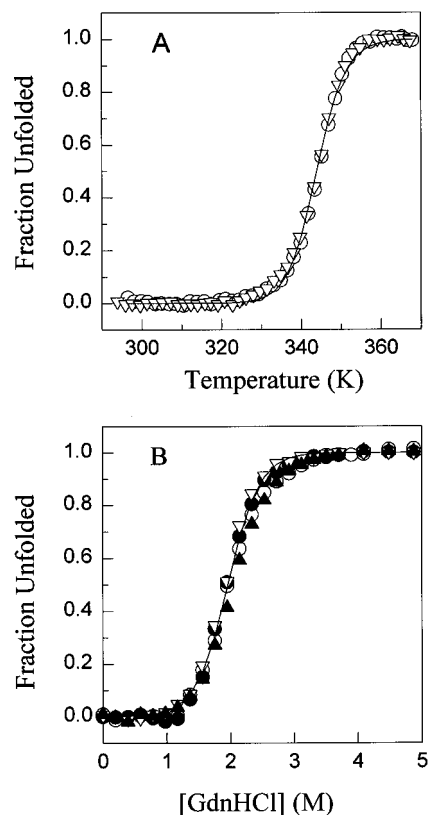


FIGURE 3: Stability of *wt* barstar in reducing and nonreducing conditions at pH 7, 25 °C. (A) Thermally-induced denaturation curves. Mean residue ellipticity at 220 nm was measured as a function of temperature in K. Thermal melts were carried out under reducing conditions in the presence of 5 mM DTT (▽) or under non-reducing conditions in the absence of DTT (○). Raw data were converted to plots of  $f_U$  versus temperature using an equation analogous to eq 1. The midpoint of the thermal transition, obtained as the temperature at which  $f_U = 0.5$ , was 345 K in each case. (B) GdnHCl-induced equilibrium denaturation curves. Mean residue ellipticity at 220 nm was measured as a function of GdnHCl concentration. Raw data were converted to plots of the fraction of protein unfolded,  $f_U$ , versus denaturant concentration, using eq 1. Barstar was prepared using buffers either containing (○, ▽) or not containing (●, ▼) 5 mM BME. Denaturation was carried out under both reducing conditions in the presence of 1 mM DTT (○, ●) and under non-reducing conditions in the absence of DTT. All four curves are coincident and a nonlinear least-squares fit of the data yields a value for  $C_m$  of 1.9 M in each case.

Thus, secondary and tertiary structures unfold concurrently upon GdnHCl-induced denaturation.

The value of  $C_m$  for *C40A* is the same as that for *wt* barstar, but the value for *C82A* is significantly lower (Table 2). When the data in Figure 7 are fitted to eq 2, the value obtained for  $m_G$  for *C40A* (-2.1 kcal mol<sup>-1</sup> M<sup>-1</sup>) was found to be marginally greater and that for *C82A* (-2.8 kcal mol<sup>-1</sup> M<sup>-1</sup>) marginally smaller than that for *wt* barstar. Conse-

Table 2: Effect of DTNB Modification on the Stabilities of *wt* Barstar, *C40A*, and *C82A* at pH 7, 25 °C<sup>a</sup>

protein	$\Delta G_U$ (kcal mol <sup>-1</sup> )	$C_m$ (M)
<i>wt</i> barstar	4.6 ± 0.2	1.92 ± 0.05
<i>C40A</i>	4.7 ± 0.2	1.95 ± 0.05
<i>C82A</i>	4.0 ± 0.2	1.68 ± 0.05
2NTB- <i>wt</i> barstar	5.9 ± 0.3	2.46 ± 0.05
1NTB- <i>C40A</i>	5.4 ± 0.4	2.25 ± 0.05
1NTB- <i>C82A</i>	4.7 ± 0.2	1.96 ± 0.05

<sup>a</sup> The value used for  $m_G$  was -2.4 kcal mol<sup>-1</sup> M<sup>-1</sup> in each case (see text). Errors shown reflect the deviations observed in at least three measurements in each case.

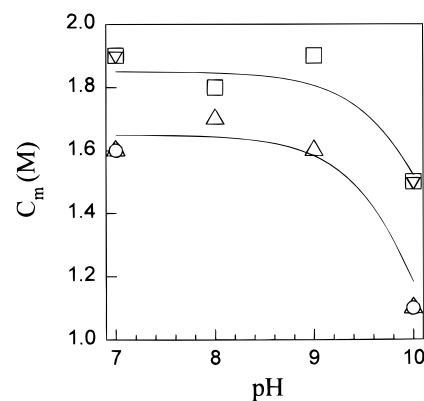


FIGURE 4: pH dependence of  $C_m$  at 25 °C (▽, □) *C40A* (△, ○) *C82A*. GdnHCl-induced equilibrium denaturation curves were obtained at the pH values shown, using both fluorescence at 322 nm on excitation at 287 nm (△, □) and mean residue ellipticity at 220 nm (▽, ○) as the probes for unfolding. The  $C_m$  value for each curve was obtained as the GdnHCl concentration at which the protein is half unfolded.

quently, the value of  $\Delta G_U$  for *C82A* (4.7 kcal mol<sup>-1</sup>) appeared to be similar to and that for *C40A* (4.1 kcal mol<sup>-1</sup>) appeared to be lower than that for *wt* barstar (4.6 kcal mol<sup>-1</sup>), and the relative stabilities appeared not to be in concordance with the relative  $C_m$  values. If the values of  $m_G$  for *C40A* and *C82A* are, however, taken to be the same as that for *wt* barstar (-2.4 kcal mol<sup>-1</sup> M<sup>-1</sup>), then the value of  $\Delta G_U$  for *C40A* (4.7 kcal mol<sup>-1</sup>) is similar to that of *wt* barstar, while that for *C82A* (4.0 kcal mol<sup>-1</sup>) is considerably lower, and the relative stabilities of the three proteins are in accordance with the measured values for  $C_m$  (Table 2).

Figure 4 shows the dependence of  $C_m$ , the midpoint of a GdnHCl-induced denaturation curve, on pH in the range 7–10.  $C_m$ , and not  $\Delta G_U$ , has been used as a measure of stability because the denaturation of *wt* barstar does not follow a two-state unfolding mechanism at pH values above 9 (Khurana *et al.*, 1995). Both mean residue ellipticity at 220 nm and intrinsic *trp* fluorescence at 322 nm were used as probes to monitor the unfolding reaction. It is seen that

there is a decrease in  $C_m$  above pH 8.0. This is in contrast with the result obtained with *C40A**C82A*, where  $C_m$  was seen to be independent of pH (Khurana *et al.*, 1995) in this pH range.

**Characterization of DTNB-Modified *wt* Barstar, *C40A*, and *C82A*.** Table 1 compares the relative activities of the DTNB-modified proteins to those of the unmodified proteins. For *wt* barstar and also for *C40A* and *C82A*, the activities of the modified and unmodified proteins can be seen to be similar. Figure 5 compares the CD spectra of DTNB-modified proteins to unmodified proteins in both the far- and near-UV regions. For *wt* barstar the mean residue ellipticity at 220 nm of the modified protein is 30% lower than that of the unmodified protein (Table 1), while for *C40A* and *C82A* there is only a marginal decrease upon modification. The near-UV CD spectra of the three modified proteins show a substantially lower signal at 275 nm. A large positive peak, which completely dwarfs the negative peak at 275 nm, is observed in each case. The positive peak is at 307 nm for *wt* barstar, at 315 nm for *C40A*, and at 305 nm for *C82A* (Figure 5). When the DTNB-modified proteins are completely unfolded in 6 M GdnHCl, the positive peak is completely absent.

DTNB-modified proteins were also obtained by reacting the fully folded proteins with DTNB for 15 h. The far- and near-UV CD spectra of the proteins modified in this manner were found to be identical to those obtained for the proteins modified by first labeling the unfolded proteins and then refolding, if the fraction of cysteine thiols that fail to be labeled in the former case (Figure 2B) was first compensated for.

The intrinsic *trp* fluorescence intensities of the modified proteins are substantially quenched in comparison to those of the unmodified proteins (Figure 6, Table 1) in both the fully folded and fully unfolded forms. In the difference UV absorbance spectra, in addition to a peak at 287 nm that is also present in the unmodified protein, each of the DTNB-modified proteins also shows a peak between 315 and 330 nm corresponding to the absorbance of the TNB label on the protein (Figure 6). The contribution of this modification to the spectrum was determined by subtraction of the spectrum of the unmodified protein from that of the modified protein. For the fully folded proteins, the TNB absorbance maxima were at 325, 327, and 316 nm for *wt* barstar, *C40A*, and *C82A*, respectively. For the fully unfolded proteins, the TNB absorbance maximum was at 335 nm for *wt* barstar and at 338 nm for both *C40A* and *C82A*. The unfolding of DTNB-modified *wt* barstar (2TNB-*wt* barstar) is accompanied by a  $\Delta\epsilon_{325}$  of  $1180 \text{ M}^{-1} \text{ cm}^{-1}$ , unfolding of DTNB-modified *C40A* (1TNB-*C40A*) by a  $\Delta\epsilon_{327}$  of  $1200 \text{ M}^{-1} \text{ cm}^{-1}$ , and unfolding of DTNB-modified *C82A* (1TNB-*C82A*) by a  $\Delta\epsilon_{316}$  of  $1060 \text{ M}^{-1} \text{ cm}^{-1}$ . Gel filtration studies showed that each modified protein eluted out at the same volume as the corresponding unmodified protein and that both the modified and unmodified proteins do not aggregate in solution, even after 24 h (data not shown).

Figure 7 shows GdnHCl-induced denaturation curves used to measure the stabilities of the modified and unmodified proteins. Far-UV CD was used to monitor unfolding. When the data for the modified proteins in Figure 7 are fitted to eq 2, the value obtained for  $m_G$  for DTNB-modified *C40A*, DTNB-modified *C82A*, and DTNB-modified *wt* barstar is  $-2.4 \text{ kcal mol}^{-1} \text{ M}^{-1}$ , which is the same as the value for

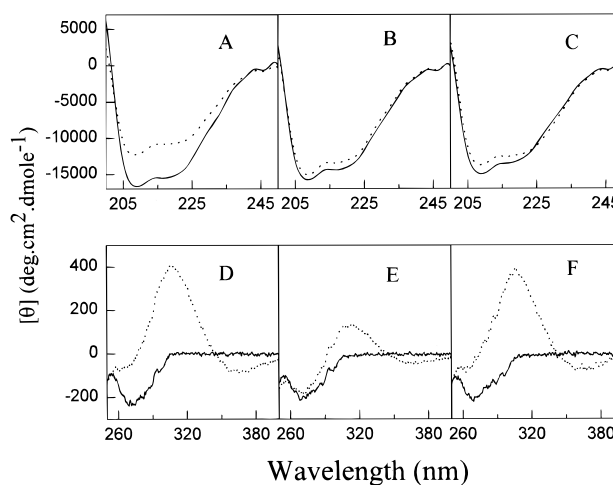


FIGURE 5: CD spectra of modified and unmodified *wt* barstar, *C40A*, and *C82A* at pH 7, 25 °C. Spectra of unmodified protein (—) and DTNB-modified (···) protein are shown. Far-UV CD spectra of (A) modified and unmodified *wt* barstar, (B) modified and unmodified *C40A*, and (C) modified and unmodified *C82A*. Near-UV CD spectra of (D) modified and unmodified *wt* barstar, (E) modified and unmodified *C40A*, and (F) modified and unmodified *C82A*.

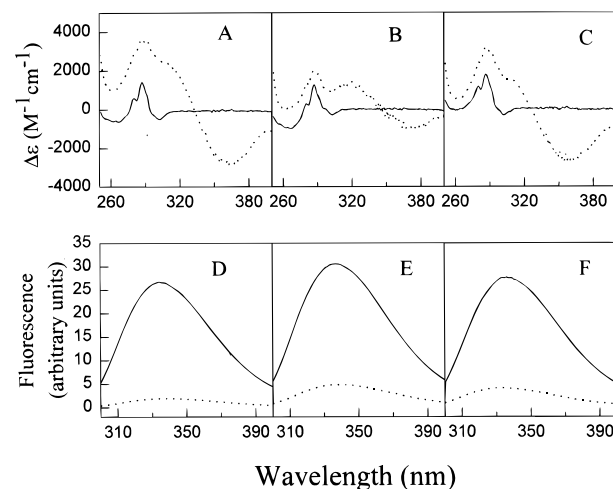


FIGURE 6: Difference UV absorbance spectra and fluorescence spectra of modified and unmodified *wt* barstar, *C40A* and *C82A* at pH 7, 25 °C. Spectra of unmodified protein (—) and DTNB-modified protein (···) are shown. In a difference UV absorbance spectrum, the difference in molar extinction coefficients of the protein in the absence and presence of 6 M GdnHCl is plotted versus wavelength. Fluorescence emission spectra were collected on excitation at 287 nm. Difference UV absorbance spectra of (A) modified and unmodified *wt* barstar, (B) modified and unmodified *C40A*, and (C) modified and unmodified *C82A*. Fluorescence spectra of (D) modified and unmodified *wt* barstar, (E) modified and unmodified *C40A*, and (F) modified and unmodified *C82A*.

unmodified *wt* barstar. Table 2 shows that the stabilities of all three modified proteins are more than those of the corresponding unmodified proteins, in terms of both  $\Delta G_U$  and  $C_m$ . When intrinsic tryptophan fluorescence at 359 nm was used to monitor unfolding, identical values for the thermodynamic parameters were obtained for *wt* barstar as well as for *C40A* and *C82A* (data not shown).

## DISCUSSION

*wt* Barstar Does Not Have a Disulfide Bond. There have been conflicting reports on whether the two cysteine residues

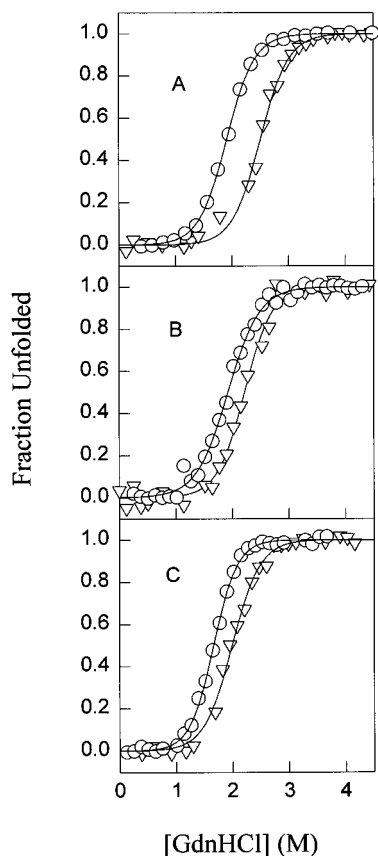


FIGURE 7: GdnHCl-induced unfolding of modified and unmodified *wt* barstar, C40A, and C82A at pH 7.0, 25 °C. The unfolding transitions were monitored by measuring mean residue ellipticity at 220 nm as a function of GdnHCl concentration. GdnHCl-induced denaturation curves of (A) unmodified (○) and DTNB-modified (▽) *wt* barstar, (B) unmodified (○) and DTNB-modified (▽) C40A, and (C) unmodified (○) and DTNB-modified (▽) C82A. The fraction of protein unfolded,  $f_u$ , is plotted versus GdnHCl concentration in each case. The solid lines through the data are nonlinear least-squares fits of the data to eq 2, and yield the thermodynamic parameters listed in Table 2 and in the text.

in barstar are involved in disulfide bond formation. In earlier studies, barstar molecules were reported to possess internal disulfide-bonds (Hartley, 1989; Schreiber & Fersht, 1993). In early NMR studies, nuclear Overhauser effect connectivities suggested that a disulfide bond may be present (Lubienski *et al.*, 1993). A later, more detailed NMR report on the solution structure of *wt* barstar, while suggesting that a disulfide bond is absent (Lubienski *et al.*, 1994), made the argument that a conformational change in the protein might make formation of an intramolecular disulfide bond possible. Indeed, *in vitro* oxidation of barstar leads to a disulfide bond containing form, which is, however, functionally inactive (Frisch *et al.*, 1995). The X-ray crystal structure of the complex of C40AC82A with barnase (Guillet *et al.*, 1993; Buckle *et al.*, 1994) also indicated that a disulfide bond was unlikely in functional *wt* barstar.

The thiol assays reported here clearly demonstrate the absence of a disulfide bond in *wt* barstar. Two thiol groups are detected per *wt* barstar molecule in both the folded and unfolded states (see Results, Figure 2). Early confusion regarding the presence or absence of a disulfide bond probably arose because of the presence of BME in the buffers used to purify the protein, which led to the formation of a mixed disulfide between barstar and BME. It is known that BME loses its protective ability after 24 h, due to air

oxidation to its disulfide form. It appears that the disulfide form of BME can then react with the free cysteine thiols in the protein to form mixed disulfide bonds. Barstar purified in the presence of BME therefore has a variable number of detectable cysteine thiols, but if purified in the absence of BME, it shows the expected two thiol groups per barstar molecule. In recent mass spectrometry studies, a fraction of barstar molecules was found to have a molecular weight approximately 75 daltons higher than expected, which could not be explained (Frisch *et al.*, 1995). The results reported here suggest that the explanation must be that these barstar molecules form a mixed disulfide with BME, which would increase their molecular weight by 75 daltons.

*Cys40 and Cys82 Have Low Water Accessibility.* The solution structure of barstar shows that Cys40 and Cys82 have water accessibilities of 5% and 25%, respectively (Lubienski *et al.*, 1994). The reaction of either DTNB or 4-PDS with the two cysteine thiols of barstar is extremely slow (Figure 2), confirming the very low solvent accessibilities of the two Cys residues. In the case of rhodanese (Pensa *et al.*, 1977) and the  $\beta$ -lactoglobulins (Phillips *et al.*, 1967), in which the cysteines are also buried, the reaction with DTNB occurs about 5-fold faster. The faster reaction of 4-PDS, compared to DTNB, with the cysteines of barstar could be due to the presence of the cysteines in a negatively charged environment. Cys40 is present in the region of the barstar molecule which interacts with barnase and which has a large density of negative charge (Buckle *et al.*, 1994).

*wt Barstar Oligomerizes in Non-Reducing and Unfolding Conditions.* Gel filtration studies (unpublished results) show that when *wt* barstar is unfolded in 6 M GdnHCl in non-reducing conditions, it oligomerizes to form a dimer and then higher molecular forms. Oligomerization is not seen in reducing conditions or in the case of C40AC82A, suggesting that it proceeds through the formation of intermolecular disulfide bonds. Negligible oligomerization is seen in gel filtration studies carried out in non-reducing conditions for the fully folded protein (unpublished results), which is expected because the cysteine residues are buried and therefore not accessible for intermolecular disulfide bond formation.

*Stability of wt Barstar Is the Same in Reducing and Non-Reducing Conditions.* Thermally induced denaturation curves for *wt* barstar, obtained under reducing and non-reducing conditions are coincident (Figure 3A). This shows that the stability of *wt* barstar is the same under both reducing and non-reducing conditions. This result contradicts an earlier study (Hartley, 1993) in which it was reported that the midpoint of the thermal denaturation curve,  $T_m$ , of *wt* barstar determined in 3 M urea, 0.2 M ammonium acetate, pH 8, was 8 °C lower in reducing conditions than in non-reducing conditions. Moreover, the  $T_m$  in the former case was similar to that of C40AC82A. That result had suggested that the higher stability in non-reducing conditions was due to the presence of a disulfide bond in *wt* barstar, which was absent in reducing conditions and in C40AC82A. When determined in 20 mM sodium phosphate or sodium borate buffer at pH 8.0 in the absence of any denaturant, the  $T_m$  of C40AC82A is, however, the same as that of *wt* barstar in reducing conditions (Khurana *et al.*, 1995) as well as in non-reducing conditions (Figure 3A). Also, *in vitro* oxidation of the cysteines in *wt* barstar leads to a disulfide bond-possessing form that is less stable and not more stable than *wt* barstar

(Frisch *et al.*, 1995), which we have shown here not to possess a disulfide bond.

*wt Barstar, C40A, and C82A Have Similar Structures and Stabilities.* The contents of secondary structure are similar in the three proteins, as evident from the far-UV CD spectra (Figure 5). The near-UV CD spectra in Figure 5 and the difference UV absorption spectra in Figure 6 indicate that the environments of the aromatic residues in the three proteins are similar. The higher fluorescence intensities of the two mutant proteins (Figure 6) suggest that both cysteines quench tryptophan fluorescence in *wt barstar*. *Cys40* quenches the fluorescence more because of its close proximity to *Trp44* (Figure 1). The similarities in the spectroscopic properties (Figures 4 and 5) and activities (Table 1) of the three proteins indicate that they have similar structures.

*wt barstar, C40A, and C82A have similar stabilities* (Table 2). Both  $\Delta G_U$ , the free energy of unfolding and  $C_m$  can be used as measures of stability. For *C40A*, in which possible interactions of *Cys40* with *Trp44* and *Ala36* (Figure 1) are lost, the values of  $C_m$  and of  $\Delta G_U$  are the same as that for *wt barstar*. For *C82A*, in which a possible interaction of *Cys82* with *Tyr47* is lost, the values of  $C_m$  and  $\Delta G_U$  are significantly lower (Table 2). Although direct fits of the denaturation curves to eq 2 indicated an increase in the value of  $m_G$  for *C40A* by 13% and a decrease for *C82A* by 17%, compared to *wt barstar*, it has been assumed in Table 2 that the value of  $m_G$  is the same for all three unmodified proteins. Such an assumption is justified because  $m_G$  is proportional to the difference between the solvent-accessible surface area in the folded state ( $A_F$ ) and that in the fully-unfolded state ( $A_U$ ) (Schellman, 1978; Agashe & Udgaonkar, 1995), and it is unlikely that either  $A_F$  or  $A_U$  is affected by the mutations. No global structural change upon mutation can be monitored by CD, fluorescence, or UV absorbance spectra, for either *C40A*, *C82A*, or *wt barstar*, in either the folded or unfolded states. The values obtained for  $m_G$  for the three modified proteins are also identical to the value obtained for unmodified *wt barstar* (see Results). The use of the same value for  $m_G$  for the two mutant proteins as that for the *wt* protein also eliminates any error in the value of  $\Delta G_U$  that might occur because of the long linear extrapolation of  $\Delta G(D)$  to  $D = 0$  (Cupo & Pace, 1983).

Deprotonation of at least one of the cysteine thiols had previously been implicated in the decrease in stability of *wt barstar* with an increase in pH above 8, which is not seen for *C40AC82A* (Khurana *et al.*, 1995). The results shown in Figure 4 indicate that both *C40A* and *C82A* become less stable as the pH is raised from 8 to 10. Thus, the decrease in stability of *wt barstar* is due to deprotonation of both cysteines and not only one. The observation that the thiol groups of the two cysteines have apparently similar  $pK_a$  values (Figure 4) is expected because both are buried to almost the same extent in *wt barstar*.

*The TNB Groups Are Buried in the Modified Proteins.* It was easy to determine whether the TNB groups introduced upon DTNB modification are buried or not in the hydrophobic interior of barstar. Upon complete folding from the unfolded state, the wavelength of maximum absorption of the TNB groups disulfide-linked to the cysteine thiols shifts from 335 to 325 nm for *wt barstar*, from 338 to 327 nm for *C40A*, and from 338 to 316 nm for *C82A*. The large blue shift in the absorption of the TNB group upon folding of each protein indicates that the TNB groups in the modified

proteins are buried in hydrophobic environments, as are the cysteine residues in the unmodified proteins.

*Structures of the DTNB-Modified Proteins.* The 30% decrease in the mean residue ellipticity at 220 nm of DTNB-modified *wt barstar* compared to unmodified *wt barstar* could be due to a contribution of the TNB group to the far-UV CD spectra. This explanation is unlikely because modification of the single cysteine in *C40A* or *C82A* does not cause a significant decrease in the far-UV CD signal. Thus, the substantial decrease in mean residue ellipticity at 220 nm must originate either from a decrease in the actual content of secondary structure or from small movements of helices 2 and 4 that would alter their relative orientation and/or separation (Cantor & Schimmel, 1980). Some actual loss of secondary structure would not be surprising because the two TNB groups are buried in the modified proteins, and their introduction into the structure increases the volume of the protein by nearly 3%. Equivalent losses in secondary structure have been reported for extreme volume mutations of  $\lambda$  repressor (Lim *et al.*, 1992), where the perturbations in volume were far less severe. Both *Cys40* and *Cys82* lie at the C-termini of helices 2 and 4, respectively, but the absence of a significant decrease in helicity of *C40A* and *C82A* upon modification makes it unlikely that a possible unfavorable interaction between the negatively charged TNB and the macrodipoles of helix 2 or helix 4 leads to helix fraying and a consequent decrease in helical content.

The near-UV CD spectra of the DTNB-modified proteins are dominated by the large positive signal between 305 and 315 nm from the TNB labels on the cysteines, which makes it impossible to determine whether the intrinsic contributions of the aromatic residues in the protein to the near-UV CD signals have been altered. The absence of the positive peak when either of the three proteins is unfolded indicates that the TNB labels in the modified proteins must be rigidly held in asymmetric environments which are not present in the unfolded state. The TNB groups must therefore be buried because it is unlikely that they could otherwise be rigidly held in asymmetric environments.

The intrinsic tryptophan fluorescence intensities of the fully folded forms at pH 7.0 for all three modified proteins are much less than those for the corresponding unmodified proteins because of non-radiative energy transfer from the tryptophans of barstar to the disulfide-linked TNB groups. The value of the Förster distance,  $R_0$ , for this donor-acceptor pair is approximately 25 Å (Wu & Brand, 1994). As expected, fluorescence intensities of the modified proteins unfolded in 6 M GdnHCl are less than those for the corresponding unmodified proteins (Table 1). The fluorescence intensities of unfolded, modified *wt barstar*, and *C82A* are substantially lower than that of unfolded, modified *C40A*, in which *Cys40* is not present. This is not surprising because the TNB label on *Cys40* is expected to be near *Trp38* and *Trp44* in the primary sequence and would be expected to quench the fluorescence strongly even when the modified protein is unfolded.

The inherent plasticity in the packing of interiors of proteins has become evident from several recent studies [reviewed in Baldwin and Matthews (1994)]. Both the main chain and side chains may adjust to a perturbation of the packing. In only a few cases have the structural adjustments been well documented (Anderson *et al.*, 1993; Ishikawa *et al.*, 1993; Lim *et al.*, 1994). It is very unlikely that the large

TNB groups are accommodated within the overall fold of barstar without accompanying movements of both the main polypeptide chain and other side chains, and the 30% decrease in mean residue ellipticity at 220 nm is probably a consequence of such structural adjustments.

**Stabilities of DTNB-Modified Proteins.** Large changes in volume in buried regions of proteins, especially in the hydrophobic cores, are usually destabilizing (Lim *et al.*, 1992; Baldwin & Matthews, 1994). The TNB groups disulfide-linked to the cysteine thiols are buried within the protein. The volume of the TNB label is equal to that of eight methylene groups. DTNB modification would therefore be expected to destabilize the protein because of (1) the severe perturbation of internal packing and (2) the burial of the negative charge of the TNB group in the hydrophobic interior of the protein. Moreover, *Cys40* is located in the region of barstar that interacts with barnase, and which has a high concentration of negative charge. The electrostatic repulsion between a negatively charged TNB group disulfide-linked to *Cys40* and its negatively charged environment would itself be expected to destabilize the protein. Also, *Cys40* is present at the C-terminus of helix 2, and *Cys82* is located just after helix 4 ends, and electrostatic repulsions between the negatively charged TNB labels on the cysteine thiols and the negative end of the helix macrodipole are also expected to be destabilizing.

Surprisingly, *wt* barstar becomes more stable by 1.3 kcal mol<sup>-1</sup> upon modification. The extents of stabilization by modification of *C40A*, in which *Cys40* is absent, and *C82A*, in which *Cys82* is absent, are similar (Table 2). Thus, modification of only *Cys40* stabilizes *wt* barstar to approximately the same extent as does modification of only *Cys82*, and the effects of the modifications of the two cysteines are additive (Table 2).

At present, the mechanism of stabilization by DTNB modification of the cysteine thiols is not known. The most likely explanation is that the structural adjustments of the main chain and side chains to the presence of the buried TNB groups lead to a better packing efficiency in buried regions, which is known to enhance stability (Anderson *et al.*, 1993; Lim *et al.*, 1994). *Cys82* lies close to *Tyr47* (Figure 1), and it is possible that there is a stabilizing interaction between the aromatic rings of *Tyr47* and the TNB label on *Cys82*. In the case of the *Ser117*→*Phe117* packing mutant of T4 lysozyme, there is both an increase in packing efficiency and the introduction of an aromatic–aromatic interaction, which stabilize the protein (Anderson *et al.*, 1993). The aromatic ring of TNB may also be involved in nonspecific stabilizing hydrophobic interactions with other residues just below the surface of the protein. In this context, engineering in a surface or near-surface hydrophobic interaction has been shown to lead to stabilization of the neutral protease from *Bacillus stearothermophilus* (Van Den Burg *et al.*, 1994). It is significant that modification of the cysteines in *wt* barstar, *C40A*, or *C82A* by iodoacetamide results in a decrease in stability (data not shown), while partial modification by BME has no effect on stability (Figure 3).

A proper understanding of the mechanism of stabilization will have to await the determination of the structures of the modified proteins by x-ray crystallography, for which crystals of the modified proteins have already been obtained (G. Ratnaparkhi and R. Varadarajan, unpublished results). An

understanding of the mechanism of stabilization may make possible a general strategy for stabilizing proteins based on chemical modification of cysteine residues that are usually found buried inside proteins.

## ACKNOWLEDGMENT

We benefitted from discussions with A. Bhuyan, M. K. Mathew, and R. Varadarajan. We thank A. Bhuyan and U. Nath for their comments on the manuscript.

## REFERENCES

- Agashe, V. R., & Udgaonkar, J. B. (1995) *Biochemistry* 34, 3286–3289.
- Agashe, V. R., Shastry, M. C. R., & Udgaonkar, J. B. (1995) *Nature* 377, 754–757.
- Anderson, D. E., Hurley, J. H., Nicholson, H., Baase, W. A., & Matthews, B. W. (1993) *Protein Sci.* 2, 1285–1290.
- Baldwin, E. P., & Matthews, B. W. (1994) *Curr. Opin. Biotechnol.* 5, 396–402.
- Bradford, M. M. (1976) *Anal. Biochem.* 72, 248–254.
- Brocklehurst, K. (1979) *Int. J. Biochem.* 10, 259–274.
- Buckle, A. M., Schreiber, G., & Fersht, A. R. (1994) *Biochemistry* 33, 8878–8889.
- Cantor, C. R., & Schimmel, P. R. (1980) *Biophysical Chemistry*, WH Freeman, San Francisco.
- Cupo, J. F., & Pace, C. N. (1983) *Biochemistry* 22, 2654–2658.
- Ellman, G. L. (1959) *Arch. Biochem. Biophys.* 82, 70–77.
- Frisch, C., Schreiber, G., & Fersht, A. R. (1995) *FEBS Lett.* 370, 273–277.
- Grasseti, D. R., & Murray, J. F. (1967) *Arch. Biochem. Biophys.* 119, 41–49.
- Guillet, V., Laphorn, A., Hartley, R. W., & Maugen, Y. (1993) *Structure* 1, 165–177.
- Hartley, R. W. (1988) *J. Mol. Biol.* 202, 913–915.
- Hartley, R. W. (1989) *Trends Biochem. Sci.* 14, 450–454.
- Hartley, R. W. (1993) *Biochemistry* 32, 5978–5984.
- Hubbard, S. J., & Argos, P. (1995) *Curr. Opin. Biotechnol.* 6, 375–381.
- Ishikawa, K., Nakamura, H., Morikawa, K., & Kanaya, S. (1993) *Biochemistry* 32, 6171–6178.
- Khurana, R., & Udgaonkar, J. B. (1994) *Biochemistry* 33, 106–115.
- Khurana, R., Hate, A. T., Nath, U., & Udgaonkar, J. B. (1995) *Protein Sci.* 4, 1133–1144.
- Liang, H., & Terwilliger, T. C. (1991) *Biochemistry* 30, 2772–2782.
- Lim, W. A., Farrugio, D. C., & Sauer, R. T. (1992) *Biochemistry* 31, 4324–4333.
- Lim, W. A., Hodel, A., Sauer, R. T., & Richards, F. M. (1994) *Proc. Natl. Acad. Sci. U.S.A.* 91, 423–427.
- Lubienski, M. J., Bycroft, M., Jones, D. N. M., & Fersht, A. R. (1993) *FEBS Lett.* 322, 81–87.
- Lubienski, M. J., Bycroft, M., Freund, S. M. V., & Fersht, A. R. (1994) *Biochemistry* 33, 8866–8877.
- Mendel, D., Ellman, J. A., Chang, Z., Veenstra, D. L., Kollman, P. A., & Schultz, P. G. (1992) *Science* 256, 1798–1802.
- Nath, U., & Udgaonkar, J. B. (1995) *Biochemistry* 34, 1702–1713.
- Pace, C. N., Shirley, B. A., & Thomson, J. A. (1989) in *Protein Structure: A Practical Approach* (Creighton, T. E., Ed.) pp 311–330, IRL Press, Oxford, U.K.
- Pensa, B., Costa, M., Pecci, L., Canella, C., & Cavallini, D. (1977) *Biochim. Biophys. Acta* 484, 368–374.
- Phillips, N. I., Jenness, R., & Kalan, E. B. (1967) *Arch. Biochem. Biophys.* 20, 192–197.
- Richards, F. M. (1977) *Annu. Rev. Biophys. Bioeng.* 6, 151–176.
- Richards, F. M., & Lim, W. A. (1994) *Q. Rev. Biophys.* 26, 423–498.
- Riddles, P. W., Blakeley, R. L., & Zerner, B. (1983) *Methods Enzymol.* 91, 49–60.
- Rose, G., Geselowitz, A., Lesser, G., Lee, R., & Zehfus, M. (1985) *Science* 229, 834–838.

- Russell, R. J. M., & Taylor, G. L. (1995) *Curr. Opin. Biotechnol.* 6, 370–374.
- Sanger, F., Nicklen, S., & Coulson, A. R. (1977) *Proc. Natl. Acad. Sci. U.S.A.* 74, 5463–5467.
- Schagger, H., & von Jagow, G. (1987) *Anal. Biochem.* 166, 368–379.
- Schellman, J. A. (1978) *Biopolymers* 17, 1305–1322.
- Schreiber, G., & Fersht, A. R. (1993) *Biochemistry* 32, 11195–11203.
- Schreiber, G., Buckle, A. M., & Fersht, A. R. (1994) *Structure* 2, 945–951.
- Shastry, M. C. R., & Udgaonkar, J. B. (1995) *J. Mol. Biol.* 247, 1013–1027.
- Shastry, M. C. R., Agashe, V. R., & Udgaonkar, J. B. (1994) *Protein Sci.* 3, 1409–1417.
- Swaminathan, R., Periasamy, N., Udgaonkar, J. B., & Krishnamoorthy, G. (1994) *J. Phys. Chem.* 98, 9270–9278.
- Van den Burg, B., Dijkstra, B. W., Vriend, G., van der Vinne, B., Venema, G., & Eijssink, V. G. H. (1994) *Eur. J. Biochem.* 220, 981–985.
- Wintrode, P. L., Griko, Y. V., & Privalov, P. L. (1995) *Protein Sci.* 4, 1528–1534.
- Wu, P., & Brand, L. (1994) *Biochemistry* 33, 10457–10462.
- Wynn, R., & Richards, F. M. (1993) *Protein Sci.* 2, 395–403.

BI9600759